

Analysis of Visible and Microwave Satellite Data for Snow  
Mapping in Alaska

Dorothy K. Hall  
Hydrological Sciences Branch, Code 974  
NASA/GSFC  
Greenbelt, MD 20771

Carl S. Benson  
Geophysical Institute  
University of Alaska  
Fairbanks, AK 99775

and

Janet Y. L. Chien  
General Sciences Corporation  
Laurel, MD 20707

**ABSTRACT**

Analysis of passive microwave Defense Meteorological Satellite Program (DMSP) Special Sensor Microwave Imager (SSM/I) data, in conjunction with Advanced Very High Resolution Radiometer (AVHRR), topographic data and vegetation maps has been undertaken for a period of time in 1989 in Alaska. The combined use of visible, near-infrared and microwave sensors to map snow will lead to an improved ability to map snow extent, albedo and water equivalent. Such data are available now from the AVHRR, and in the future, from the Earth Observing System Moderate Resolution Imaging Spectroradiometer (MODIS). Passive microwave sensors are necessary in order to augment visible and near-infrared sensors which cannot acquire data through cloudcover and darkness. Results show a strong dependence of the microwave brightness temperature on topography, land cover and vegetation biomass. Also, the influence of persistent meteorological conditions on snow temperature is hypothesized as an explanation for a brightness-temperature anomaly observed during the winter in the northern foothills of the Brooks Range, Alaska.

## **Introduction**

Because of its high albedo, low thermal conductivity and large surface coverage, snow plays an important role in the Earth's climate system. Improved snow-cover data are required as input to hydrologic and general circulation models (Rango, 1993). Additionally, snow is an important water resource in many parts of the globe.

The ability to map global snow cover will improve significantly in the Earth Observing System (EOS) era with the launch of the Moderate Resolution Imaging Spectroradiometer (MODIS) and the Multifrequency Imaging Microwave Radiometer (MIMR) in the late 1990s and early 21st century. MODIS will have bands in the visible, near-infrared and thermal-infrared parts of the spectrum that will enable delineation of snow cover, and snow/cloud discrimination (see Riggs et al., this volume). Snow albedo may also be calculated using MODIS and Multi-angle Imaging Spectro-radiometer (MISR) data. The MIMR will enable snow mapping through cloud cover and darkness. In addition, other snowpack parameters will be measurable using MIMR data, such as snow water equivalent and grain size. Used together, MODIS, MIMR and MISR data will enable the production of global-scale maps of snow extent, water equivalent and albedo.

In this paper, we discuss efforts to improve our understanding of Defense Meteorological Satellite Program/Special Sensor Microwave Imager (DMSP/SSM/I) snow maps of Alaska by employing NOAA Advanced Very High Resolution Radiometer (AVHRR), vegetation and topography data sets to compare with the microwave-derived results. The suitability of the 'greenness index' map derived using NOAA/AVHRR data is also discussed in comparison with a vegetation map of Alaska. Results show a strong dependence of the microwave brightness temperature on topography, land cover and vegetation biomass. This further confirms results of work in other geographic regions demonstrating the influence of forests and topography on the microwave signature of snow.

## **Background**

NOAA visible and near-infrared satellite data have been used since the late 1960s to map snow cover in the Northern Hemisphere (Matson, 1986). These maps have demonstrated the large variability in extent of snow between years. While the NOAA maps have been extremely useful, various factors adversely affect the accuracy of the snow maps: 1) snow and clouds cannot be distinguished definitively; 2) snow cannot be mapped through cloud cover and darkness; and 3) snow in densely-forested areas cannot be mapped reliably (Dewey and Heim, 1982; Robinson, 1993).

Passive microwave data have also been used to map Northern Hemisphere snow cover (Kunzi et al., 1982; Chang et al., 1987), at a resolution of more than 30 km since 1978. The passive microwave-derived maps also provide an indication of snow-water equivalent in some areas. Parameters affecting the passive-microwave response of snow include: water equivalent, density, grain size, temperature, surface roughness and forest-cover fraction and type (Pulliainen et al., 1993). As with the visible and near-infrared data, there are also significant difficulties in the use of passive-microwave data for snow extent and thickness mapping (Rango et al., 1979). Problems are inherent in the interpretation of the data, including: 1) the coarse resolution of the passive microwave data is not suitable for regional snow studies; 2) mapping snow in densely-forested areas is difficult; and 3) derivation of snow-water equivalent is dependent upon snow and land cover characteristics.

Vegetation has been found to confuse the normally-inverse relationship between microwave brightness temperature and snow depth in dry snowpacks (Hall et al., 1982; Hallikainen et al., 1984; Foster et al., 1991; Chang et al., 1991 and Hallikainen and Jolma, 1992), and various schemes have been devised to attempt to eliminate or lessen the influence of vegetation over snow-covered areas. For example, Foster et al. (1991) found that in the boreal forest in Saskatchewan, the bias between measured and remotely-sensed snow water equivalent could be reduced by 22 percent by using an algorithm that took percent forest cover into account.

#### **Data Sets and Methodology**

SSMI data from January to June 1989 covering most of Alaska were acquired. Also acquired were AVHRR data covering approximately the same area and time period. Due to cloud contamination and darkness, much of the AVHRR data are not usable in the present format. Figure 1 is a 16 March 1989 AVHRR image showing snow cover in Alaska. Most of the lower half of Alaska is also covered by clouds.

We have examined two sources of vegetation data and topographic data of Alaska. The vegetation data are: 1) a U.S. Geological Survey vegetation map of Alaska (Kuchler, 1985), and 2) a NOAA/AVHRR - derived "greenness index" which was obtained from the Eros Data Center, Sioux Falls, South Dakota. The NOAA data represent an average of 2 weeks of AVHRR data, beginning on 2 July 1990.

Topographic data, used in this study, may be obtained from the National Geophysical Data Center in Boulder, Colorado which distributes a compact disc entitled "Geophysics of North America." Topographic data of North America reside on that CD. The data provide average elevations on a 5-minute grid.

The vegetation map of Alaska (Kuchler, 1985) has been digitized and registered to the passive microwave, AVHRR and topographic data of Alaska. This permitted our study of the effects of different land covers on the brightness temperatures of Alaska in winter.

According to Kuchler (1985), only ten major vegetation types exist in Alaska; the vegetation is limited to a few types due to the harsh environmental conditions. One of the outstanding characteristics of the vegetation in Alaska is its uniformity over large areas. North of the Brooks Range, the Arctic Coastal Plain is composed of watersedge tundra and cottonsedge tundra. Watersedge tundra is found on the coast of the Arctic Ocean and cottonsedge tundra is found farther inland. Watersedge tundra consists of very wet, non-woody vegetation while cottonsedge tundra occurs at somewhat higher elevations and in areas of more rugged topography, and contains clumps of woody tussocks which are not found in the areas of watersedge tundra. Significant amounts of watersedge tundra occur elsewhere in Alaska, most notably in the Yukon-Kuskokwim Peninsula, and in the northern part of the Seward Peninsula of Alaska. Elsewhere, except in and adjacent to the mountains, forest cover predominates, consisting of black spruce, spruce-birch, hemlock and alders (Kuchler, 1985). Black spruce and spruce-birch forests occupy most of the Alaska's interior, between the Brooks Range and the Alaska Range.

The AVHRR bands, located in the visible and near-infrared parts of the spectrum, may be used to construct maps of 'greenness' for North America. The algorithm used to derive the maps is:

$$\text{NDVI} = \frac{\text{IR} - \text{VIS}}{\text{IR} + \text{VIS}} \quad [1]$$

Where NDVI is the normalized difference vegetation index which is related to vegetation biomass (Tucker, 1986). IR is data acquired from the near-infrared part of the spectrum, and VIS is data acquired from the visible part of the spectrum. The quantity and vigor (or photosynthetic activity) is related closely to vegetation type.

#### **Regional snow conditions in Alaska**

Different snow types characterize the three major climatic regions of Alaska. Tundra snow, a dry, wind-packed, high-density shallow snow is found on the Arctic Slope of Alaska. Taiga snow, a dry, low-density, largely-recrystallized snow is found in the Interior. Wet, maritime snow is found in the southern coastal regions of Alaska (Benson, 1980).

Tundra snow, which lasts for about nine months each year, is further characterized by a low-density, large-grained, depth-hoar layer at the base of the snowpack. Taiga snow occurs in the forested interior of Alaska which is snow covered for approximately six months each year. Relatively warm soils at the base of the snowpack, and low, ambient air temperatures, produce steep temperature gradients (often  $>1^{\circ}\text{C}/\text{cm}$ ) which, in turn, produce steep vapor pressure gradients and lead to the development of depth hoar (Trabant and Benson, 1972; Sturm, 1991). Depth hoar at the base of the taiga snowpack is quite well developed, often composing most of the total snowpack by the end of winter. Because the coastal mountains and lowlands of southeastern and south-central Alaska receive heavy precipitation, the maritime snowpack can be up to 15 m thick, and in contrast with the tundra and taiga snow, may be at or near the freezing point and is often moist or wet (Benson, 1980).

Vegetation can have an important effect on snow cover. Vegetation introduces complex voids and channels which, when combined with the vertical temperature gradients, produce convective action leading to horizontal temperature gradients at the snow/substrate interface (Sturm, 1992). These gradients vary over horizontal distances of a few meters. Sturm (1992) shows that heat flow from tree wells created in snow can be more than twice that of undisturbed snow. In forested watersheds, these local effects of vegetation on the snow cover have an influence that is regional in scale, and may thus influence the satellite-derived passive microwave brightness temperature. Although the emissivity of the dense vegetation has the greatest effect on brightness temperature.

#### **Air temperatures and snow conditions in Alaska - January through June 1989**

During January of 1989 in central Alaska, there were about 48 cm of snow on the ground as measured at the National Weather Service (NWS) Station in Fairbanks (NWS, 1989). Temperatures in the early part of the month were low, but decreased dramatically by the latter half of the month (Figure 2). On 28 January, the maximum air temperature was  $-42^{\circ}\text{C}$ . Then a dramatic warming event occurred, and by 12 February, the maximum air temperature had increased to  $2^{\circ}\text{C}$ . By this date, the snow depth was 61 cm. A similar pattern occurred in northern and southwestern Alaska as seen in the meteorological records from Barrow and Bethel, respectively, however, snow depths in Barrow and Bethel were less than those in the Interior.

#### **Passive Microwave brightness temperatures in Alaska-January through June 1989**

Some persistent brightness temperature patterns are visible in the SSMI winter images of Alaska. Low 37-GHz horizontally-polarized brightness temperatures are found in

the Brooks Range, and in the Yukon/Kuskokwim Peninsula. Within the Arctic Coastal Plain in the northern foothills of the Brooks Range, there is an area of even lower brightness temperature that has been observed previously and reported by Hall et al. (1991) and referred to as a brightness-temperature anomaly. Generally higher brightness temperatures are found to occur between the Brooks Range and the Alaska Range.

Other areas where persistent zones of low brightness temperatures are found are located in south-central Alaska in the heavily-glacierized Chugach Mountains, and the arcuate-shaped Alaska Range. The low brightness temperatures in those areas are due to the low emissivity of the glacier ice.

### **Results and Discussion**

The boundary between the watersedge and cottonsedge tundras on the Arctic Coastal Plain is evident on Kuchler's vegetation map, the greenness index map, and the AVHRR data. Because of the difference in elevation, the boundary is also visible on the topographic data. Watersedge tundra is found in flat, poorly-drained areas. Cottongrass tundra is found in areas of greater relief and consists of tussocks and some woody parts. Watersedge tundra areas found in southwestern Alaska also have low 37-GHz brightness temperatures as seen on the SSMI data.

On the Arctic Coastal Plain of Alaska, the  $T_B$  decrease inland is probably related to the greater surface roughness of the cottonsedge (tussock) tundra. The cottonsedge tundra, with greater surface roughness than the watersedge tundra, probably traps more snow, thereby increasing the scattering of the 37-GHz radiation and thus lowering the microwave brightness temperature. This may explain why brightness temperatures are generally lower in the cottonsedge versus the watersedge tundra areas.

In the Interior, 37-GHz brightness temperatures are higher than on the Arctic Coastal Plain even though the snow is deeper. One might expect microwave emission to be lower due to greater scattering in deeper snow. The higher brightness temperatures are probably related to the forest cover in the Interior. High biomass emits more microwave energy causing higher brightness temperatures. Also, the dense forests may mask the underlying snow (Hall et al., 1982; Goodison et al., 1986; Chang et al., 1991). In the barren areas, devoid of much vegetation and underlain by frozen ground, brightness temperatures are generally low.

When the AVHRR-derived greenness index map is compared with Kuchler's vegetation map of Alaska, there are similarities as well as differences. The watersedge and the cottonsedge tundras on the Arctic Coastal Plain are clearly visible on

both data sets. Dryas meadows are observable on Kuchler's map but are less obvious on the greenness map. The spruce-birch and black-spruce forests of the Interior are not easily distinguished on the greenness map, but are distinguished on Kuchler's map. The glacier ice in the Brooks Range, Alaska Range and in the mountains of southern and southeastern Alaska shows up clearly on both maps. Kuchler's map is considered, for the purpose of this study, to be the "ground truth" information on vegetation in Alaska.

The preliminary conclusion is that the greenness index map is a good measure of vegetation biomass, but less accurate than Kuchler's map for distinguishing vegetation or forest type. This is based on using the AVHRR-averaged data from the 2-week time period that we selected. Perhaps future studies utilizing different channels and/or time periods are likely to provide different results. While forest-cover type is important in understanding passive-microwave response, biomass is of greater importance, and thus the AVHRR greenness index maps represent a useful data set.

Strong winds in the northern foothills of the Brooks Range may contribute to the anomalously-low brightness temperatures found there. Opposing winds meet in the northern foothills of the Brooks Range, causing the inversion layer that prevails over the northern part of the Arctic Coastal Plain in the winter to be more strongly developed. Thus the area can be quite calm in winter compared to other parts of the Arctic Coastal Plain. In an inversion, air temperature increases with height in the lower part of the atmosphere resulting in a lower surface temperature at the bottom of these areas, relative to surrounding areas that are not influenced by the inversion. This could cause a lower brightness temperature because the brightness temperature is strongly related to the physical temperature of the feature being sensed. A simplification of the relationship between emissivity,  $E$ , and brightness temperature,  $T_B$ , is given by Zwally and Gloersen (1977):

$$E = T_B/T \quad [2]$$

where  $T$  is the physical temperature of the object. The area of low brightness temperature found in the northern Brooks Range foothills area appears to move around throughout the winter and between years. This may be because the actual location of the 'wind shadow' migrates as weather conditions change and as the location and intensity of the surface inversion changes.

In early January (1989), average daily air temperatures in the Alaskan interior (Fairbanks) varied from about  $-17^{\circ}\text{C}$  to  $-10^{\circ}\text{C}$  (Figure 2). The snow cover was continuous. When the air temperatures dropped suddenly in mid-to-late January,

below  $-40^{\circ}\text{C}$ , brightness temperatures became dramatically lower, averaging about  $225^{\circ}\text{K}$  on January 7-9, to  $180^{\circ}\text{K}$  on January 27-29, in the Interior. In the northern foothills of the Brooks Range, the zone of anomalously-low brightness temperature expanded and 37-GHz emission within the zone decreased (Figure 3). If our theory is correct, that means that the size of the wind shadow increased as the inversion layer became better developed due to calmer conditions by January 27-29. By February 6-8, the zone of anomalously-low brightness temperature became more diffuse, perhaps meaning that the inversion was dissipating as air temperatures and winds increased.

By early February, the air temperatures increased dramatically all over Alaska. A corresponding increase in brightness temperature is observed in the SSMI data acquired on 6-8 February. The brightness temperatures on the Arctic Coastal Plain increased by  $10-20^{\circ}\text{K}$ . Still greater brightness temperature increases ( $35-45^{\circ}\text{K}$ ) are seen in the Interior. The area of anomalously-low brightness temperature on the Arctic Coastal Plain got much smaller and almost disappeared during the warming event (Figure 3), but re-formed as temperatures decreased again in mid February.

### **Conclusion**

Results show that passive microwave data of snow cover cannot be interpreted properly without analysis of topographic and vegetation data. The influence of topography is twofold: 1) topography influences vegetation type, and 2) topography influences physical temperature of the near-surface. Vegetation data acquired from different sources are in general agreement.

Persistent meteorological influences, like surface inversions that form over snow in the winter, will influence the snow temperature. This, in turn, may influence the passive microwave brightness temperature of snow. One such area may be present in the northern foothills of the Brooks Range in northern Alaska.

In this paper, we have not addressed the snow parameters known to affect brightness temperature such as grain size and water equivalent, but have concentrated on land-cover, topographic and meteorological aspects that influence brightness temperature. As these background factors become understood, an improved ability to map snow cover and to determine snow depth will ensue.

### **Acknowledgements**

The authors would like to thank Jim Tucker, NASA/GSFC for providing AVHRR data of Alaska, Penny Masuoka, University of Maryland, for digitizing the vegetation map, Hugh Powell, General Sciences Corporation, for processing SSMI data, and Jim Foster, NASA/GSFC for discussions relating to the

interpretation of the passive microwave data and for his review of the paper.

## References

- Benson, C.S., 1980: Alaska's snow, Weatherwise, V. 33, pp. 202-205.
- Chang, A.T.C., J.L. Foster and D.K. Hall, 1987: Nimbus-7 derived global snow cover parameters, Annals of Glaciology, V.9, pp.39-44.
- Chang, A.T.C., J.L. Foster and A. Rango, 1991: Utilization of surface cover composition to improve the microwave determination of snow water equivalent in a mountain basin, International Journal of Remote Sensing, V.12, pp.2311-2319.
- Dewey, K.F. and R. Heim, Jr., 1982: A digital archive of Northern Hemisphere snow cover, November 1966 through December 1980, Bulletin of the American Meteorological Society, V.63, pp.1132-1141.
- Foster, J.L., A.T.C. Chang and A. Rango, 1991: Derivation of snow water equivalent in boreal forests using microwave radiometry, Arctic, V.44, pp.147-152.
- Goodison, B., I. Rubinstein, F.W. Thurkettle and E.J. Langham, 1986: Determination of snow water equivalent on the Canadian prories using microwave radiometry, in Modeling Snowmelt-Induced Processes, IAHS Publ. No. 155, pp.163-173.
- Hall, D.K., J.L. Foster and A.T.C. Chang, 1982: Measurement and modeling of microwave emission from forested snowfields in Michigan, Nordic Hydrology, V.13, pp.129-138.
- Hall, D.K., M. Sturm, C.S. Benson, A.T.C. Chang, J.L. Foster, H. Garbeil and E. Chacho, 1991: Passive microwave remote and in situ measurements of arctic and subarctic snow covers in Alaska, Remote Sensing of Environment, V.38, pp.161-172.
- Hallikainen, M.T., 1984: Retrieval of snow water equivalent from Nimbus-7 SMMR: effect of land-cover categories and weather conditions, IEEE Journal of Oceanic Engineering, V.OE-9, pp.372-376.
- Hallikainen, M.T. and P.A.. Jolma, 1992: Comparison of algorithms for retrieval of snow water equivalent from Nimbus-7 SMMR data in Finland, Transactions of the IEEE Journal on Geoscience and Remote Sensing, V.30, pp.124-131.
- Kunzi, K.F., S. Patil and H. Rott, 1982: Snow-cover parameters retrieval from Nimbus-7 scanning

- multichannel microwave radiometer (SMMR) data, IEEE Transactions on Geoscience and Remote Sensing, V.20, pp.452-467.
- Kuchler, A.W., 1985: Potential Natural Vegetation, U.S.G.S. Map from National Atlas, sheet no.89.
- Matson, M., C.F. Ropelewski and M.S. Varnadore, 1986: An atlas of satellite-derived northern hemisphere snow cover frequency, U.S. Dept. of Commerce, NOAA/NWS, GPO, 75 p.
- NWS (National Weather Service), 1989: Climatological Data of Alaska, January - June 1989.
- Pulliainen, J., J.-P. Karna and M. Hallikainen, 1993: Development of geophysical retrieval algorithms for the MIMR, IEEE Transactions on Geoscience and Remote Sensing, V.31, No.1, pp.268-277.
- Rango, A., A.T.C. Chang and J.L. Foster, 1979: The utilization of spaceborne microwave radiometers for monitoring snowpack properties, Nordic Hydrology, V.10, pp.25-40.
- Rango, A., 1993: Snow hydrology processes and remote sensing, Hydrological Processes, V.7, pp.121-138.
- Riggs, G.A., D.K. Hall, V.V. Salomonson and J. Barker, this volume: The developing Moderate Resolution Imaging Spectroradiometer (MODIS) snow-cover algorithm, Proceedings of the 50th Eastern Snow Conference.
- Robinson, D.A., 1993: Recent trends in Northern Hemisphere snow cover, Fourth Symposium on Global Change Studies, 17-22 January, 1993, Anaheim, CA, American Meteorological Society, pp.329-334.
- Sturm, M., 1991: The role of thermal convection in heat and mass transport in the subarctic snow cover, CRREL Report 91-19, 82 p.
- Sturm, M., 1992: Snow distribution and heat flow in the Taiga, Arctic and Alpine Research, V.24, pp.145-152.
- Trabant, D. and C.S. Benson, 1972: Field experiments on the development of depth hoar, Geological Society of America Memoir, V.135, pp.309-322.
- Tucker, C.J., 1986: Maximum normalized difference vegetation index images for sub-Saharan Africa for 1983-1985, International Journal of Remote Sensing, V.7, pp.1383-1384.

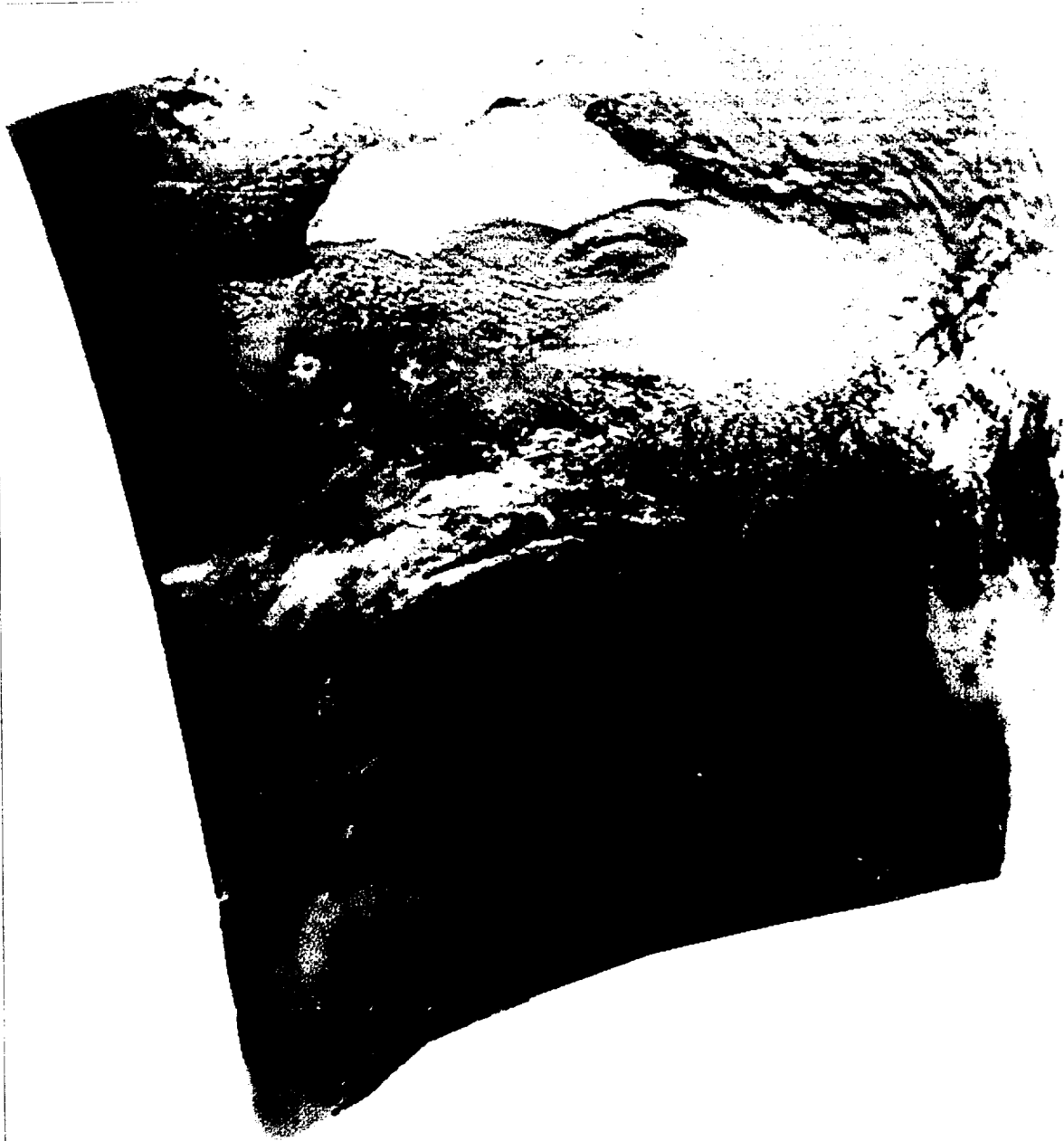
Zwally, H.J. and P. Gloersen, 1977: Passive microwave images of the polar regions and research applications, Polar Record, V.18, pp.431-450.

## Figures

1 NOAA/Advanced Very High Resolution Radiometer (AVHRR) image acquired on 16 March 1989, using channels 2, 4 and 5, showing most of Alaska. Snow cover is visible in the northern part of the State, while the southern part is cloud covered.

2 Maximum daily temperatures for 3 stations in Alaska from January 1 - June 30, 1989.

3 Line drawing showing the changes in the extent of the lowest brightness temperatures in Alaska. Areas with brightness temperatures  $<170^{\circ}\text{K}$  are shown. Note the expansion of the low brightness temperature areas in late January when air temperatures decreased.

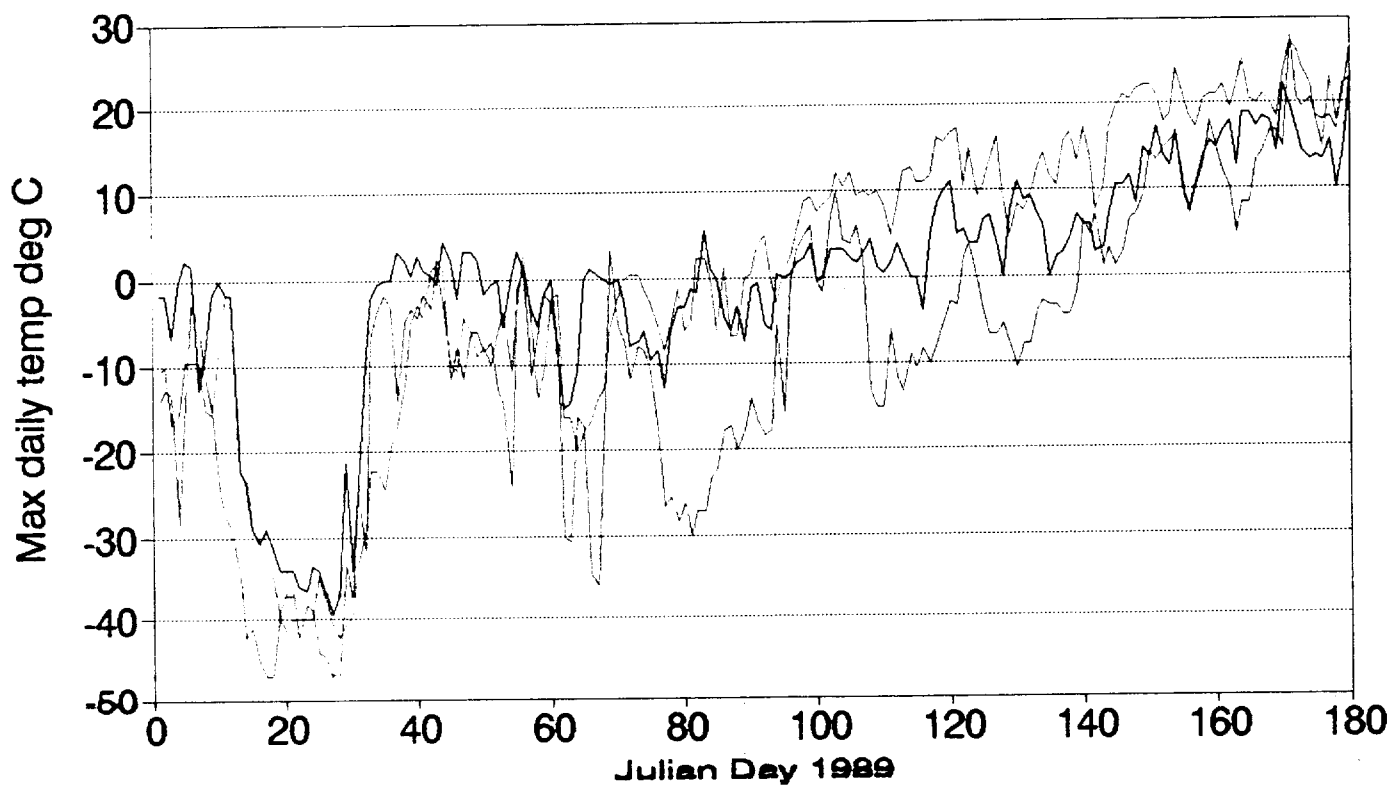


AVHRR DATA 03/16/89

band 2, 4, & 5

Figs. 2+3  
are being  
drawn at our  
graphics lab

# Alaska



— Fairbanks — Umiat — Bethel

- 7-9 Jan 1989  
-- 27-29 Jan  
... 6-8 Feb

